A Systematic Approach of a Various Natural Acid-Base Indicator on Fruits Using CNN

Nithya C. [1], Elarmathi S.[2], Kavya G. S.[3], Divya Bharathi G.[4], Kumarganesh S.[2] and Malathi Murugesan[5]

[1]*Department of CSBS, Knowledge Institute of Technology, Salem 637504, Tamil Nadu, India*
[2]*Department of ECE, Knowledge Institute of Technology, Salem 637504, Tamil Nadu, India*
[3]*Department of BME, Paavai College of Engineering, Namakkal 637018, Tamil Nadu, India*
[4]*Department of CSE, Mahendra Institute of Technology, Namakkal 637503, Tamil Nadu, India*
[5]*Department of ECE, E.G.S. Pillay Engineering College, Nagapattinam 611002, Tamil Nadu, India*

Keywords: Bayesian Optimization, Citrus, CNN Regression, Fluorescence, Fruits, MobileNetV2, Acid-Base Indicators, pH.

Abstract: To determine the ripeness of citrus fruits, one of the most widely used indicators of fruit development is the Brix/acid ratio, which is the ratio of the fruit's sugar or soluble solids content to its acid content. A single spectrum can be subjected to successive applications of a diverse set of statistical models known as SGFP. These statistical models comprise particular models for differentiation of product categories, fruit type differentiation amongst citrus varieties, separation of multiple fruit types, and characterization of compositional differences between two sets of items that are otherwise highly similar. The Brix/acid ratio was estimated using fluorescence spectroscopy, a technique that is not only fast and sensitive but also very affordable. After the orange peels were removed, each peel's fluorescence value was calculated. The suggested system is unusual in that it analyses the fluorescence spectrum using a convolutional neural network (CNN). When performing fluorescence spectroscopy, a matrix known as an excitation and emission matrix (EEM) can be created. For every excitation and emission wavelength, the fluorescence intensity is noted in this matrix. A CNN was then used to perform a regression in order to determine the Brix/acid ratio of the juice that was collected from the meat. To do this, the EEM was viewed as a picture (CNN regression).

1 INTRODUCTION

Various types of synthetic chemical indicators are accessible for the different kinds of titrimetric investigations. PH indicators are measures of acidity and baseness. Acid-base indicators are chemicals (dyes) whose colours vary when the pH of their environment changes. They are often weak bases or acids, which means they only dissociate and give ions in solution to a small extent. Pure volumetric analysis is one of the principal techniques of quantitative methodologies. The equivalence point calculation in titrimetry is often based on the end point of the titration. One of the applications of this kind of analysis is classical titrimetry, where the end of a point is detected by adding some compounds to the analyse solution that cause chromatic changes, immediately after to each point. These compounds are often called indicators. Different types of titrimetric studies have several types of indicators, most of which are either very weak organic acids or very weak organic bases that respectively accept or release electrons. Morimoto T, et al., 1994, Although there are modern automated titration devices that identify the equivalent point between reagaging species, indicators are widely used for simple titration in academic and research labs. Momin A.M., et al., 2010, Thus, the price of commercial indicators is very high, and some have proved to have deleterious effects on users as well as the risk of polluting the environment. These properties motivated the search for supplementary predictors based essentially on natural forcings.

One of the most well-known and widely eaten types of fruit all around the globe is citrus. Citrus production was the second-highest of all fruits in Japan in 2015, with Satsuma mandarin (Citrus unshiu Marc.) being the most popular cultivar. Citrus must

C., N., S., E., S., K. G., G., D. B., S., K. and Murugesan, M.
A Systematic Approach of a Various Natural Acid-Base Indicator on Fruits Using CNN.
DOI: 10.5220/0013882600004919

In *Proceedings of the 1st International Conference on Research and Development in Information, Communication, and Computing Technologies (ICRDICCT'25 2025) - Volume 2*, pages 330-336
ISBN: 978-989-758-777-1

not only be consistently available but also of an ever-increasingly high quality to satisfy customer demand. To begin, the harvest period of citrus should be carefully decided by taking into consideration the maturity of the fruit in order to satisfy demand. Reid M.S. 2002, This is due to the fact that when citrus fruit is harvested with a high degree of maturity, it is more prone to being damaged by mechanical means or infected by pathogens during the postharvest handling process. On the other hand, if it hasn't been matured properly, it won't have a pleasant taste or look, and it may not even be sellable.

Cary P.R; Iglesias D.J, 2007, Changes in size, shape, colour, hardness, and the Brix/acid ratio have all been used frequently to determine the maturation level of citrus fruit. Since brix and acidity measure the quantity of sugar or soluble solids present and the amount of acid present, respectively, they are especially important parameters. Kimball D, 1991, Their ratio, sometimes referred to as the Brix/acid ratio, is one of the most widely used indicators to assess the ripeness of fruit in addition to the quality of the juice.

Figure 1: Sample Images of Forty Types of Fruits.

Kondo N, et al, 2000 The fruits were planted in a revolving motor shaft at a speed of three revolutions per minute (rmp), and a brief video recording of twenty seconds was recorded for each class. These stills are taken directly from the video. Because of the different lighting circumstances, an algorithm was used to eliminate the backdrop from each of the photographs. The example photos of fruit that were taken are shown in Figure 1. The exact calculation of the Brix/acid ratio is used to identify the optimal time to harvest the crop. In the past, the interior quality was evaluated based on the characteristics of the object's exterior, such as its dimensions, form, and mass, as well as its colour. However, the Brix and acidity levels could not be accurately estimated. Antonucci et al. used a portable visible-near infrared (VIS-NIR) spectrophotometer to determine the Brix and acidity values; however, this method is very expensive. Tamilarasi M, et al, 2024 Another method that has recently gained popularity is fluorescence spectroscopy, which is a rapid, sensitive, and cost-effective technology.

The researchers Muharfiza et al. looked into the viability of fluorescence spectroscopy as a method for determining the stage of maturation reached by Satsuma mandarins. The fluorescence features were observed and measured throughout the phases of development and maturation, and then contrasted with the conventional maturity indicator known as the Brix/acid ratio. Muharfiza; et al., 2017 According to the findings of the research, the Brix/acid ratio was linked to the fluorescence peaks of amino acids and chlorophyll, and the peak intensity was useful for estimating the Brix/acid ratio. However, as of yet, no quantitative analysis of the accuracy of the Brix/acid ratio calculation has been conducted. In addition, the assessment was based on just two of the fluorescence peaks that a citrus peel really possesses, despite the fact that a citrus peel actually contains several fluorescence peaks. In addition, the estimate accuracy might be improved by taking into account data other than the peaks of the fluorescence spectrum, such as the shoulder, unevenness, and troughs of the spectrum Wang, et al, 2010.

2 EXPERIMENTAL SETUPS

The purpose of this study is to develop an optimum classification model that can recognise and distinguish between the many kinds of fruits. Python 3.0 running on Windows 10 was used to build the suggested model, and the system setup included an i7 CPU and 16 gigabytes of random access memory (RAM). As can be seen in Figure 2, the model is evaluated with a variety of records abstracted from a 2 by 2 confusion matrix.

- Macro Average: This macro average is calculated by computing F-1 for each label and then averaging the scores, ignoring the fraction of the dataset that corresponds to the labels.
- Weighted Average: The one that calculates F-1 of each label and averages them weighted by the proportion of the dataset represented by each label.

2.1 Estimation of the Brix/Acid Ratio with CNN Regression

In the present study, one of the most conventional type of CNN was used. In this particular CNN, there are three different types of layers the fully-connected layer, pooling layer, and the convolution layer. Sugiyama J, et al, 2013 CNN regression was performed by moving the regression layer to the very last layer to get the Brix/acid estimate. 1) Mean square error refereed as a loss function. We then adjusted the weight of each filter and bias to minimize mean square error due to the difference between the estimated and actual Brix/acid ratio and the estimated value.

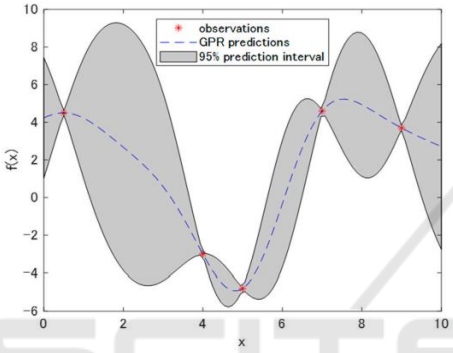

Figure 2: An Illustration of a Five-Observation Gaussian Process Regression (Dotted Line). the 95% Prediction Interval Is Shown by the Patched Area.

In Figure 2, a dotted line represents the results of the predictions made using a Gaussian process regression. Barbedo J.G.A, 2018 The estimated value of the function with the most probable outcomes is shown in this line. The area that has been patched with grey may contain the function's value. This illustrates that the percentage is 95%. The Gaussian distribution may be described using each graph that was extracted in the vertical direction for a particular x value.

2.2 Flowers, Plants and Fruits Materials

Red cabbage, tulip petals, rose petals, rosa damascene, red onion skin, curcuma, cinnamon, ginger, saffron, black pepper, red pepper, yellow pepper, coffee, quince leaf, strawberry, sour berry, cornelian cherry, carrot, green walnut, parsley, coriander, borage, and allium ampeloprasum were prepared from Agricultural Research Center of Tabriz. Flowers, plant leaves and petals, and the skins of fruits and vegetables are all included as examples Suh, et al., 2018. After being rinsed completely under running tap water and then cleansed with distilled water, the samples were allowed to air dry before being pulverised using a mechanical blender.

Then, the score with respect to the p-th region by averaging the response over the modalities:

$$S_p = \sum_{m=1}^{M} S_{m,p} \quad (1)$$

Given this threshold, the precision (P), recall (R) and F1 score are computed as:

$$Precision\ (\mathrm{P}) = \frac{TP}{TP+\mathrm{FP}} \quad (2)$$

$$Recall(R) = \frac{TP}{TP+FN} \quad (3)$$

$$F1\ Score = \frac{2PR}{P+R} \quad (4)$$

where T_P is the numeral value of true positives (correct detections), F_P is the numeral value of false positives (false detection), F_N is the number of false negatives (miss) and T_N is the numeral value of true negatives (correct rejection).

2.3 Chemicals Required

All of the chemicals were of analytical reagent quality and were obtained from Sigma-Aldrich Chemical (carbon tetrachloride, chloroform, ethanol, methanol, toluene, and hydrochloric acid) and Merck (all other compounds). Water that had undergone two distillations was used to make each solution.

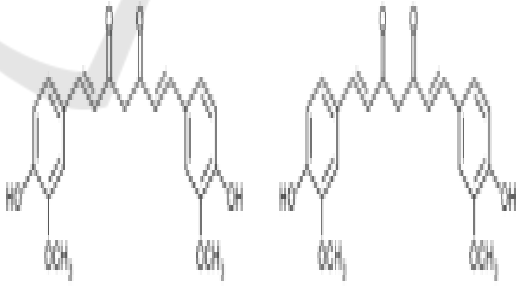

Figure 3: Chemical Construction of Curcumin in Enol (A) and Keto (B).

2.4 Apparatus

Reagent bottle, weighing balance, spatulas, hot plate, shaker, oven, electric blender, test tubes, test tube support, droppers, 50 mL buretes, wash bottle, beaker, spatula, pipettes, pipette filler, funnel, clamp support, tissue, magnetic stirrer, watch glass, volumetric cylinders of 25 mL and 50 mL, conical

flask, pH paper, magnetic stirrer, watch glass pH meter (electronic - Switzerland model OHAUS2100), measuring cylinders, and glass and calomel electrodes.

2.5 Extraction Preparation of Flowers, Plants and Fruits in Various Solvents

To explore the extraction efficiencies of the five organic solvents, two grams of the sample powder were mixed with fifty millilitres of carbon tetrachloride, chloroform, ethanol, methanol, and toluene as solvents by stirring the mixture for forty-eight hours. The solution was vigorously agitated and stirred to ensure the entire component would dissolve. The extract is filtered by suction through strainer paper with the aid of a Buchner funnel and collected in a filter flask. All aqueous abstract were used after evaporation as natural pointer in acidimetric and alkalimetric measurements. One-fifth of the volume of the original abstract was extracted. The extract was protected from light by storing it in a container with a lid in the dark.

3 RESULTS AND DISCUSSION

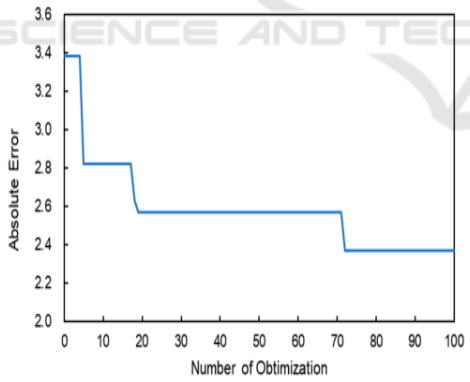

Figure 4: Relationship Between the Number of Optimizations and the Brix/Acid Ratio Estimate's Smallest Absolute Inaccuracy.

Figure 4 illustrates the relationship between the minimal absolute error in the Brix/acid ratio and the number of parameter modifications. As more improvements were carried out, the estimate's lowest absolute error decreased to a smaller value. Results from the same optimization method were quite similar when it was repeated.

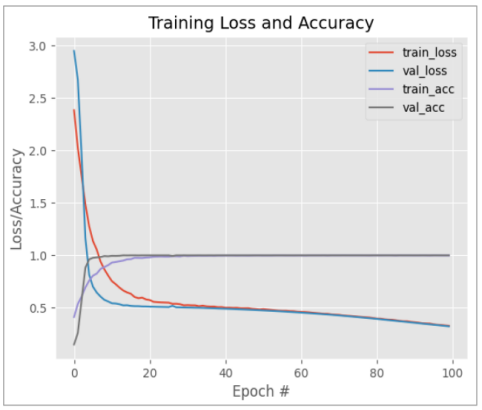

Figure 5: Training Accuracy and Loss in Terms of Training and Validation of Tl-Mobilenetv2 Model.

Figure 5 also includes a representation of the suggested model's training loss. The illustration shows that the training loss is relatively significant at the beginning of the training phase since the model has not yet been presented with the data. This is illustrated in the image. But, with time the model learns to understand the pictures and begins to recall them; as a result, the training loss progressively decreases. It is possible to see that the training loss approaches 0.6 during the first 20 iterations and then decreases noticeably with each subsequent iteration beyond that point. The training loss has reached 0.3 by the time the 100th iteration has passed, which indicates that the model has the qualities of a good one.

Table 1: Assessment Value of Brix/Acid Ratio.

S. No	Assessment Method	AEE of Brix/Acid Ratio
1.	Two peaks of poly methoxy flavone	6.20
2.	Two peaks of Tryptophan and Chlorophyll	4.48
3.	PCR (Principal Component Regression)	4.03
4.	Proposed method (CNN regression)	2.47

Together with the absolute error of the present CNN regression and the previous estimate methods, Table 1 displays the absolute error of the Brix/acid ratio.

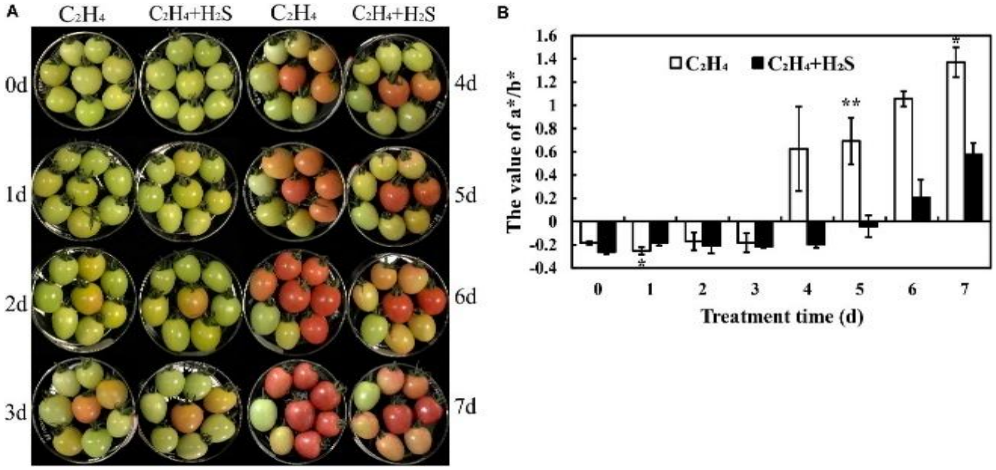

Figure 6: The Phenotypic Alteration of Post-Harvest Tomato Fruits Treated With C2h4 or C2h4-H2s.

(A) Morphological change of tomato fruit after harvest. (B) The tomato post-harvest storage a/b value regarding colour parameter changes after C2H4 or C2H4-H2S treatment. The magenta to green colour range is represented by the a* value whereas the yellow to blue colour range is represented by the b* value. Values are the means standard deviations (n = 3). All of the above experiments were performed at room temperature and ~85–90% relative humidity. The symbols and * indicate a p 0.05 and p 0.01, respectively, significant difference between C2H4 and C2H4-H2S.

Figure 6A depicts the colour change of tomato fruit over the post-harvest storage period. On the 0th day, all tomato fruits are clearly seen to be at the green-yellow (G-Y, 30% yellow skin) stage. During the first and second days, some C2H4-induced tomatoes are in the green-orange (G-O, 50% orange skin) stage, but tomato fruits are practically in the G-Y stage due to the C2H4 + H2S co-treatment. The colour change was indicated using an a/b value, as seen in Figure 6B. Over the storage time, the a/b values of the two treatment groups increased, whereas the a/b value of the H2S + ethylene treatment group remained lower than that of the ethylene treatment alone. Hence, further H2S treatment may reduce tomato colour change and postpone tomato fruit ripening during post-harvest storage.

Table 2: The Factors Score of All the Metabolites by Principal Component Analysis in Tomato Fruits.

Metabolites	Component 1	Component 2	Component 3
Content of titratable acid (C2H4 + H2S)	0.975	0.18	0.150
Protease activity (C2H4)	-0.95	0.12	0.272
Content of chlorophyll b (C2H4 + H2S)	0.948	0.101	-0.25
Content of starch (C2H4 + H2S)	0.939	0.156	-0.228
Content of titratable acid (C2H4)	0.895	0.427	0.240
Content of Anthocyanidin (C2H4 + H2S)	-0.88	0.191	0.276
Protease activity (C2H4 + H2S)	-0.871	0.276	0.376
Content of total phenol (C2H4 + H2S)	-0.806	0.535	0.133
Content of chlorophyll a (C2H4)	0.796	0.522	-0.109
Content of reducing sugar (C2H4)	0.783	0.420	-0.537

Content of reducing sugar (C2H4 + H2S)	0.776	0.252	-0.529
Content of total phenol (C2H4)	-0.697	0.427	0.237
Content of chlorophyll (C2H4)	0.69	0.645	0.267
Content of Anthocyanidin (C2H4)	-0.633	0.581	0.445
Content of flavonoid (C2H4 + H2S)	0.221	0.952	-0.274

This is a principal component analysis study presented in Table 2 and seen in Figure 7. 77% of the variance was provided by the first three components (PC1, PC2, and PC3 with respective contribution rates being 47.64, 38.42, and 6.3%. The major components described by PC1 were TA, protease activity and starch. The major contributor to PC2 was Flavonoid, chlorophyll b, and amylase activity, while ascorbic acid accounted for PC3.

Table 3: Anthocyanidic Compounds, Obtained from the Analysis in the Uhplc-Esi-Q-Orbitrap-Ms / Ms.

Compound Name	Fragment Weight (m/z)	Condensed Formula	Retention time (Min)
Cyanidin - Diglucoside	611.18 m/z	$C_{27}H_{31}O_{16}^{+}$	19.1 min
Cyanidin – Monoglycoside	433.11 m/z	$C_{21}H_{21}O_{11}^{+}$	20.2 min
Pelargonidin – Diglucoside	595.18 m/z	$C_{27}H_{31}O_{15}^{+}$	19.5 min
Cyanidin	287.06 m/z	$C_{15}H_{11}O_{6}^{+}$	19.1 min
Pelargonidin	271.06 m/z	$C_{15}H_{11}O_{5}^{+}$	19.5 min

Table 4: Values of Pk1 As a Function of Ph Stability in the Presence of Oxygen and Light from the Extract Punica Granatum L.

Number	Ph	Absorbance	Pk1
1	6	0.455	a = Ain
2	6.5	0.461	b=Hin-
3	7	0.473	-
4	7.5	0.55	-
5	8	0.578	-
6	1.5	1.018	a = Ain
7	10	0.305	b=Hin-

The characterization of the extract of the fruit Punica granatum L. was carried out using a UV-Vis spectrophotometer, and the investigation of the extract's stability in the presence of light lasted for a period of seven days (Spectro quant Pharo 300). The different performance analyses of a UHPLC system are shown in Figures 9 and 10. And the PH scale is shown in figure 11 below.

Table 5: Stability in the Presence of Light As a Function of the Absorbance of the Two Glass Bottles (Colorless and Amber).

		Colorless glass bottle	Amber glass bottle
Days	Dates	Absorbance	Absorbance
0	15-May-2017	0.77	0.77
1	16-May-2017	0.593	0.366
2	17-May-2017	0.495	0.439
3	18-May-2017	0.496	0.452
4	19-May-2017	0.565	0.452
5	20-May-2017	0.533	0.416
6	23-May-2017	0.497	0.371

4 CONCLUSIONS

A fluorescence measurement of extracted citrus peel was carried out, and a regression using CNN was executed in order to provide an accurate estimate of the Brix/acid ratio of juice taken from the flesh. It was decided to treat the EEM that was generated from the fluorescence measurement as a picture, which made the CNN regression possible. As a consequence of this, the absolute error in the Brix/acid ratio was assessed to be 2.48, which is a significant improvement compared to the values produced by the various other approaches in the earlier investigations. Not only was this a suitable strategy for the prediction, but we also did Bayesian optimization in order to choose hyper-parameters in the deep neural network. Both of these things contributed to the

accuracy of the forecast. Because of the optimization, the parameters were able to be determined automatically and accurately. This was made possible by the optimization. In addition, it wasdiscovered that the optimization process itself was responsible for the high level of accuracy. In future work, a mobile-based application will be further enhanced using a larger number of different fruits, which aims to lead to a wider range of fruit classification.

REFERENCES

Antonucci F, Pallottino F, Paglia G, Palma A, D'Aquino S, Menesatti P, Non-destructive estimation of mandarin maturity status through portable VIS-NIR spectrophotometer. Food Bioprocess. Technol. 2011, 4, 809–813.

Barbedo J.G.A, Factors influencing the use of deep learning for plant disease recognition. Biosyst. Eng. 2018, 172, 84–91.

Barbedo J.G.A, Impact of dataset size and variety on the effectiveness of deep learning and transfer learning for plant disease classification. Comput. Electron. Agric. 2018, 153, 46–53.

Cary P.R, Citrus Fruit Maturity; MPKV: Rahuri, India, 1974; p. 26.

Christensen J, Povlsen, V.T, Sorensen J, Application of fluorescence spectroscopy and chemometrics in the evaluation of processed cheese during storage. J. Dairy Sci. 2003, 86, 1101–1107.

Deng, L.Hinton, G, Kingsbury, B. New types of deep neural network learning for speech recognition and related applications: An overview. In Proceedings of the 2013 IEEE International Conference on Acoustics, Speech and Signal Processing (ICASSP), Vancouver, BC, Canada, 26–31 May 2013; pp. 8599–8603

Iglesias D.J, Cercós M, Colmenero-Flores J.M Naranjo, M.A, Ríos, G Carrera E, Ruiz-Rivero O, Lliso I, Morillon R, Tadeo F.R, et al. Physiology of citrus fruiting. Braz. J. Plant Physiol. 2007, 19, 333–362.

Itakura K, Hosoi F, Estimation of tree structural parameters from video frames with removal of blurred images using machine learning. J. Agric. Meteorol. 2018, 74, 154–161.

Kimball D, Citrus Processing: Quality Control and Technology; Springer Science & Business Media: New York, NY, USA, 1991; p. 55.

Kondo N, Ahmad U, Monta M, Murase H, Machine vision based quality evaluation of Iyokan orange fruit using neural networks. Comput. Electron. Agric. 2000, 29, 135–147.

Maggiori E, Tarabalka Y, Charpiat G, Alliez P, Convolutional neural networks for large-scale remote-sensing image classification. IEEE Trans. Geosci. Remote Sens. 2017, 55, 645–657.

Miao S, Wang, Z.J, Liao, R. A CNN regression approach for real-time 2D/3D registration. IEEE Trans. Med. Imaging 2016, 35, 1352–1363. [CrossRef]

Ministry of Agriculture, Forestry and Fisheries. The Situation Surrounding Fruits. Available online: http: //www.maff.go.jp/j/seisan/ryutu/fruits/attach/pdf/index -57.pdf (accessed on 20 November 2018).

Momin A.M, Kondo N, Ogawa Y, Shiigi T, Kurita M, Ninomiya K, Machine vision system for detecting fluorescent area of citrus using fluorescence image. Proc. IFAC 2010, 43, 241–244.

Morimoto T, Chikaizumi S, Hashimoto Y, Intelligent quality control of fruit storage factory. J. Shita 1994, 6, 191–196.

Muharfiza; Riza A.F.D, Saito Y, Itakura K, Kohno Y, Suzuki T, Kuramoto M, Kondo N, Monitoring of Fluorescence Characteristics of Satsuma Mandarin (Citrus unshiu Marc.) during the Maturation Period. Horticulturae 2017, 3, 51.

P. Elayaraja, Kumarganesh S, K. Martin Sagayam & J. Andrew, (2024), "An automated cervical cancer diagnosis using genetic algorithm and CANFIS approaches" International Journal of Technology and Health Care, 32 (4), pp. 1-17, https://content.iospres s.com /articles/technology-and-health-care/thc230926.

Reid M.S., Maturation and maturity indices. In Postharvest Technology of Horticultural Crops; University of California Division of Agriculture and Natural Resources Publication: Oakland, CA, USA, 2002; pp. 21–28.

Selvalakshmi B, Hemalatha K, Kumarganesh S & Vijayalakshmi P (2025), Performance analysis of image retrieval system using deep learning techniques. Network: Computation in Neural Systems, 1–21. https://doi.org/10.1080/0954898X.2025.2451388.

Sugiyama J, Tsuta M, Discrimination and quantification thechnology for food using fluorescence fingerprint. Nippon Shokuhin Kagaku Kogaku Kaishi 2013, 60, 457–465.

Suh, H.K, Ijsselmuiden J, Hofstee J.W, van Henten E.J, Transfer learning for the classification of sugar beet and volunteer potato under field conditions. Biosyst. Eng. 2018, 174, 50–65.

Tamilarasi M, Kumarganesh S, K. Martin Sagayam and Andrew J, (2024) "Detection and Segmentation of Glioma Tumors Utilizing a UNet Convolutional Neural Network Approach with Non-Subsampled Shearlet Transform" Journal of Computational Biology, 31 (8) pp. 1-16, https://www.liebertpub.com /doi/full/10.1089/cmb.2023.0339.

Wang, X, Cao, L, Yang S.T, Lu F, Meziani M.J, Tian L, Sun K.W, Bloodgood, M.A.; Sun, Y.P. Bandgap-Like strong fluorescence in functionalized carbon nanoparticles. Angew. Chem. Int. Ed. 2010, 49, 5310–5314.